

# Lab report

## K223 Nuclear $\gamma$ - $\gamma$ Angular Correlations

Chenhuan Wang and Harilal Bhattarai

August 18, 2020

In this experiment, we investigate nuclear properties of cobalt nuclei via angular correlation. With scintillation detectors, we measure number of coincidence in dependence on angle between two photons. There is strong anisotropy in coincidence rate present. The measured data are fitted with the theoretical prediction function and calculated the angular correlation coefficients:  $A_{22} = 0.0849 \pm 0.0057$  and  $A_{44} = -0.0002 \pm 0.0063$ . Closer investigation reveals that measured values differ from prediction by  $4\sigma$ . Other types of cascade are excluded almost 100%.

### 1 Introduction

In a cascade gamma decay of nuclei a non-isotropic angular distribution can be measured due to non-equilibrium spin state; however, in thermal equilibrium net orientation of all spin states is zero due to gamma ray distribution of nuclei is isotropic. Thus, the angular correlation between two gamma rays emitted during the cascaded gamma decay of the nucleus is due to the unequal spin states distribution in the intermediate states [1]. The main motive of the experiment is set up the experiment and investigate nuclear properties of  $^{60}\text{Co}$  via angular correlation of  $\gamma - \gamma$  cascades[1].

### 2 Theory

**Angular correlation** of gamma rays of multipole moments  $L_{1,2}$  from  $\gamma$ - $\gamma$  cascade  $I_i \rightarrow I \rightarrow I_f$  is defined as

$$W(\theta) = 1 + \sum_{k=2, \text{ even}}^{k_{\max}} A_{kk} P_k(\cos \theta) \quad (1)$$

with  $A_{kk}$  (known given the information of nucleus) coefficients,  $P_k(\cos \theta)$  the Legendre polynomials, and  $k_{\max} = \min(2I, 2L_1, 2L_2)$ [2]. Alternatively, equivalent definition is sometimes used [3]

$$W(\theta) = 1 + \sum_1^l a_i \cos^{2i} \theta \quad (2)$$

**Coefficient**  $A_{kk}$  is determined, generally with mixed multipole components  $L'_n$  and  $L_n$  ( $n = 1, 2$ ), by

$$A_{kk} = A_k(L_1 L'_1 I_i I) A_k(L_2 L'_2 I_f I) \quad (3)$$

$$A_k(L_n L'_n I_{i,f} I) = \frac{F_k(L_n L_n I_{i,f} I) + 2\delta_1(\gamma) F_k(L_n L'_n I_{i,f} I) + \delta_1^2(\gamma) F_k(L'_n L'_n I_{i,f} I)}{1 + \delta_1^2(\gamma)} \quad (4)$$

$$F_k(LL'I'I) = (-1)^{I'+I-1} [(2L+1)(2L'+1)(2I+1)(2k+1)]^{1/2} \times \begin{pmatrix} L & L' & k \\ 1 & -1 & 0 \end{pmatrix} \left\{ \begin{matrix} L & L' & k \\ I & I & I' \end{matrix} \right\} \quad (5)$$

$$\delta_1(\gamma) = \frac{\langle I | L'_1 \pi'_1 | I_{i,f} \rangle}{\langle I | L_1 \pi_1 | I_{i,f} \rangle} \quad (6)$$

with round brackets being  $3j$ -symbols and curly brackets  $6j$ -symbols[2]. Their value can be easily found tabulated, e.g. in [4] and [5].  $\delta_n(\gamma)$  quantifies the mixing of two multipole moments and should be determined by some other methods. If we assume  $L'_n = L_n + 1$  (this is reasonable because of selection rules), then there are 7 quantum numbers to nail down the coefficients:  $I_i, I, I_f, \delta_{1,2}, L_{1,2}$ [2].

**Example** with  $0 \rightarrow 1 \rightarrow 0$   $\gamma$ - $\gamma$  cascade. Since the first and last states are of spin 0, the multipolarities of emitted photon must be 1, thus dipole-dipole radiation. According to [3]

$$W(\theta) = 1 + \cos^2(\theta) \quad (7)$$

Plot of this angular correlation can be found in figure 1.

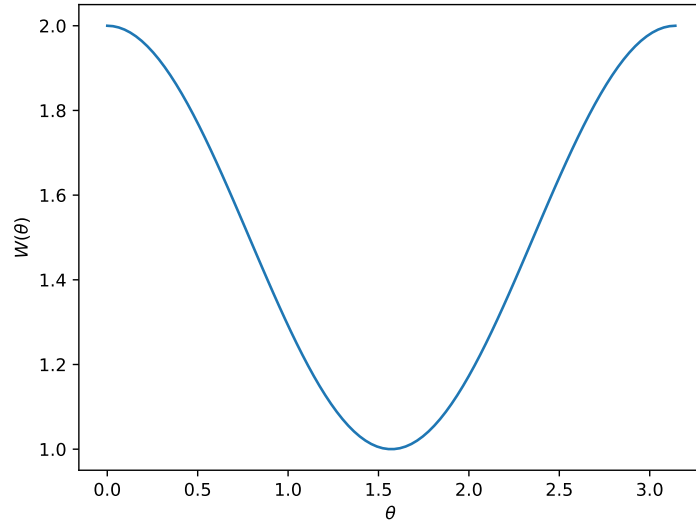


Figure 1: Angular correlation of hypothetical 010 cascade

**Hyperfine structure** can have influence on the angular correlation, since with quantization axis along the direction of first photon the first photon will cause transitions among the  $m$ -states. Thus in the end, the direction of second photon is altered. The perturbed angular

correlation is given as

$$W(k_1, k_2, t) = \sum_{m_i, m_f, m_a, m'_a} \langle m_f | H_2 \Lambda(t) | m_a \rangle \langle m_a | H_1 | m_i \rangle \langle m_f | H_2 \Lambda(t) | m'_a \rangle^* \langle m'_a | H_1 | m_i \rangle^* \quad (8)$$

where  $H_{1,2}$  represents the interaction between nucleus and radiation field and  $\Lambda(t)$  is an unitary operator describing influence of extranuclear perturbation.  $k_1$  and  $k_2$  are wave vector of photons. [2].

**Information** can be obtained from measurement of  $\gamma$ - $\gamma$  angular correlations (without extranuclear perturbation): spin angular momenta of excited states, the multipole orders, and the relative multipole composition of radiative transitions[6]. With extranuclear perturbation, we can in addition extract  $g$ -factor and quadrupole momentum of intermediate state. Internal fields of solids, liquids, and metal crystals can be investigated. And some changes in atomic shell is possible to study [2].

## 3 Experimental setups

### 3.1 Key components

**Scintillation detector** is used to detect ionizing radiation in general. Here we have gamma radiation. The purpose of scintillator is to lower photon energy via photoelectric effect, Compton scattering, and pair production [7]. It is then connected to photomultiplier tube (PMT) to generate signals.

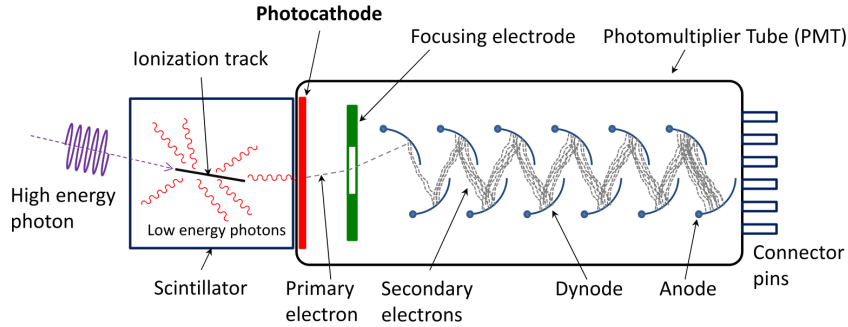


Figure 2: Scintillator with PMT [8]

**Fast-slow coincidence** is the technique to measure the ionizing radiation separately. The "slow" part will determine the energy of incoming radiation. And the "fast" part is used to measure the time as precisely as possible, since the photomultiplier will be brought to saturation and the height of the pulse is not proportional to radiation energy any more [9].

**SCA** stands for single channel analyzer. Basically it is advanced version of simple discriminator, as one can set both upper-level (ULD) and lower-level discriminator (LLD) for SCA. It reads the input pulse and check whether it is within the preset limits or not. If it is, SCA will produce a uniform digital signal. When applied to PMT, the height of pulse corresponds

to energy of radiation. If SCA is built in after PMT, we are essentially picking out photons within the SCA window. Thus the name [10].

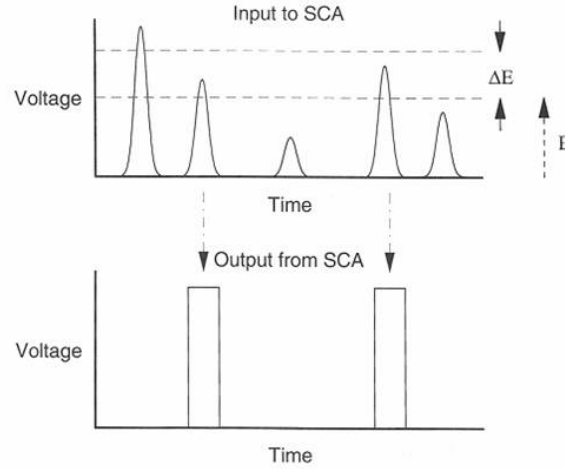


Figure 3: Single Channel Analyzer [8]

**CFD** stands for constant fraction discriminator. As its name suggests, it gets triggered at some preset fraction of maximal amplitude, in order to reduce "walk". In simplest form, CFD works by splitting input signals, inverting one of them, and adding delay to the other. In the end, by combining these two together, we get logic signal with minimal walk [11].

**Expected Spectrum** of  $^{60}\text{Co}$  would predominantly consists of 0.31 MeV  $\beta$ -line and 1.1732 MeV, 1.3325 MeV  $\gamma$ -line [12]. Its  $\gamma$ -spectrum can be found in 4, where one can see two clear peaks corresponding to the  $\gamma$ -radiations and some background because of various effects, like pair production (higher  $E$ ), Compton scattering (mid  $E$ ), and photoelectric effect (low  $E$ ) [7].

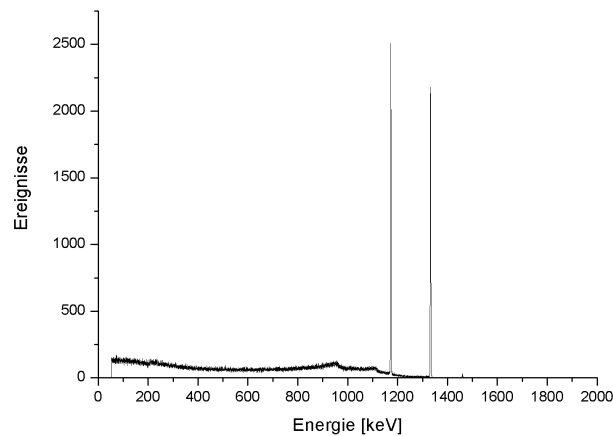


Figure 4:  $^{60}\text{Co}$   $\gamma$ -spectrum [13]

## 4 Task for preparation

### 4.1 Which distances to pick?

Obviously, the count (rate) should be proportional to the solid angle ignoring the anisotropy of radiation. This assumption should not bring too much influence to the results, as long as the size of detection is accounted for in final analysis as (systematic) error. In [2], true count rate is given by

$$N_i^t(\theta) = Mp_i\Omega_i\epsilon_i \quad (9)$$

with  $M$  the number of nuclear integrations per unit time,  $p_i$  the probability that this integration is selected,  $\Omega_i$  is solid angle in unit  $4\pi$ , and  $\epsilon_i$  the detector efficiency. According to formula of solid angle, it means that

$$N_i^t(\theta) \propto \frac{1}{r_i^2} \quad (10)$$

Follow the same principle, true number of coincidence can be written as [2]

$$C^t(\theta) = Mp_1p_2\Omega_1\epsilon_1\Omega_2\epsilon_2\epsilon_c K(\theta) \quad (11)$$

where  $\epsilon_c$  is the efficiency of coincidence unit and  $K(\theta)$  is the directional correlation function.  $K(\theta)$  is basically the "measured" version of  $W(\theta)$ , i.e. what we have in the real world. The coincidence rate is then  $C^t(\theta)/N_1^t(\theta)$  thus

$$\frac{C^t(\theta)}{N_1^t(\theta)} \propto \frac{1}{r_2^2} \quad (12)$$

The angular "asymmetry" is represented as the coefficients  $A_{kk}$ . With correction factor, we write

$$A_{kk} = \frac{A_{kk}^{\text{exp}}}{Q_{kk}} \quad (13)$$

And it can be calculated by [2]

$$Q_{kk} = Q_k(1)Q_k(2) \quad (14)$$

$$Q_k(i) = \frac{J_k(i)}{J_0(i)} \quad (15)$$

$$J_k(i) = \int_0^{\pi/2} \epsilon_i(E, \alpha) P_k(\cos \alpha) \sin \alpha \, d\alpha \quad (16)$$

$$\epsilon(E, \alpha) = 1 - \exp\{-\tau(E)X(\alpha)\} \quad (17)$$

with  $\tau(E)$  the total absorption coefficient and  $X(\alpha)$  the distance traversed in the crystal.

The correction factor will certainly affect the error of angular correlation function, multiplicatively to be specific.

According to table in [2],  $h = 10$  cm would provide the most precise measurement, since the  $Q_i$ 's are closer to 1. So in the actual experiment, one can try to measure the event rate in a short time period. Then the distance should be chosen, so that enough data will be taken in the given time but still have maximal precision.

## 4.2 Which angles to pick?

The angular correlation function is given in the form of [1]

$$f(\theta) = A(1 + B \cos^2 \theta + C \cos^4 \theta) \quad (18)$$

It can be rewritten with  $\alpha = B + C$  and  $\beta = B - C$ ,

$$f(\theta) = A \left( 1 + \frac{\alpha + \beta}{2} \cos^2 \theta + \frac{\alpha - \beta}{2} \cos^4 \theta \right) \quad (19)$$

Predicted values for  $A_{22}$  and  $A_{44}$  without mixing are given in [2]. Then the predicted correlation function is

$$\begin{aligned} W(\theta) &= 1 - \frac{A_{22}}{2} + \frac{3}{8}A_{44} + \left( \frac{3}{2}A_{22} - \frac{15}{4}A_{44} \right) \cos^2 \theta + \frac{35}{8}A_{44} \cos^4 \theta \\ &= 0.952412 + 0.118875 \cos^2 \theta + 0.039813 \cos^4 \theta \end{aligned} \quad (20)$$

Need to "scale" it, so that 0.9524 gets absorbed in  $A$ . Then we have

$$B = 0.124815, C = 0.041802$$

Plot correlation with these two coefficients with slight variation, we have figure. 5 From it,

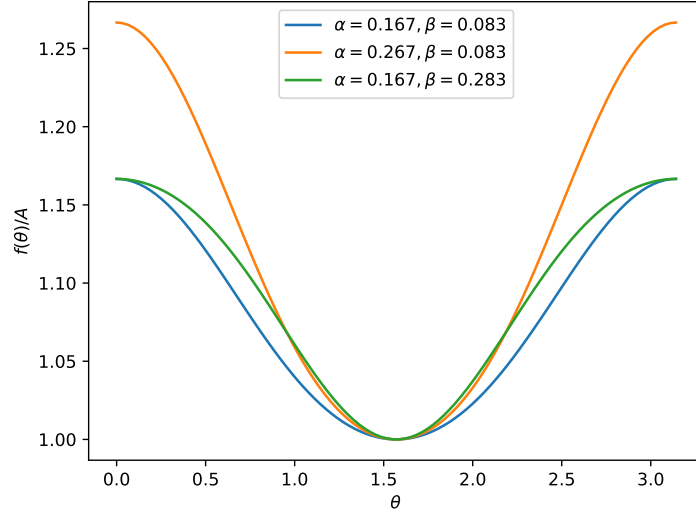


Figure 5: Correlation with different  $\alpha$  and  $\beta$

it is clear that to determine  $\alpha$ , we need in principle only one point ( $\theta = 0$  or  $\theta = \pi$ ). But determination of  $\beta$  requires small increments in angle between 0 and  $\pi/2$ .

## 4.3 How to correct for de-adjustment?

In actual setup, the source might not lie perfectly in the center of circle of detectors. It will certainly cause a distortion in data, since extra "angular correlation" will be introduced. Depending on in which direction the source is off from the center of circle, the angular correlation could have an obvious asymmetry or just simply gets stretched out. To correct this, count rates of two detectors needs to be recorded. Coincidence rate should be normalized against these count rates.

## 5 Analysis

Firstly the data needs to be corrected because of random coincidences and misalignment of the setup. Random coincidence rate  $\dot{R}$  is simply subtracted from the coincidence rate. In calculation of error of count rate, error of random coincidence is considered as well.

$$\dot{R} = (2.218 \pm 0.061) \text{ s}^{-1} \quad (21)$$

It is thought to be acceptable to just use one random coincidence rate for all angles, since it has no angular dependence. Effects of misalignment on random coincidence need to be considered. That is why the data get correction for misalignment after this step.

In figure. 6, one can see a clear asymmetry in count rate of the mobile detector. This can be easily explained by source not being in the center of the setup. True coincidence rate should be anti-proportional to count rates in figure. 6. Since measured angular correlation function is determined up to a proportional constant anyway, the normalization factor  $\kappa$  is chosen to be the fraction of count rate at smallest angle and count rate at respective angle.

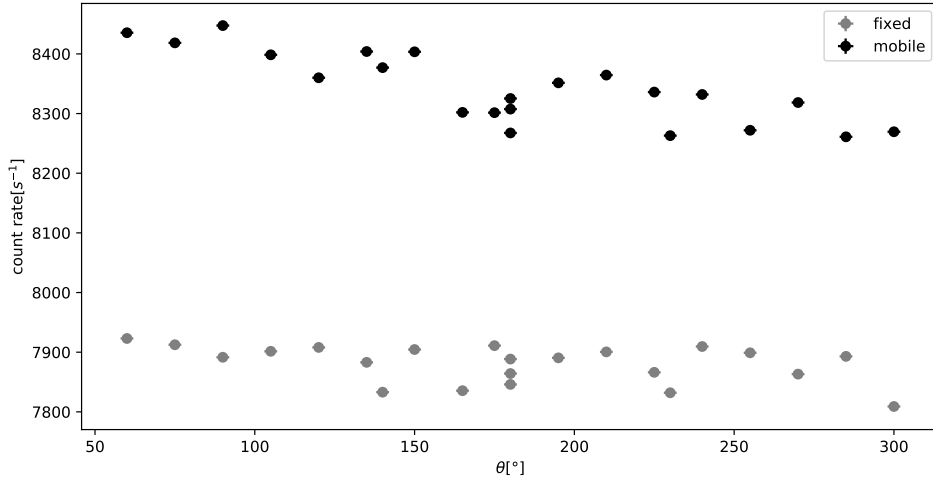


Figure 6: Raw count rate

Coincidence rates are normalized against the raw count rate with  $\kappa$ , in order to counter misalignment. True coincidence rate  $\dot{C}_{\text{true}}$  is calculated via

$$\dot{C}_{\text{true}} = \kappa \cdot (\dot{C}_{\text{measured}} - \dot{R}) \quad (22)$$

During experiment, the setup and its environment might (inevitably) change, i.e. temperature. Measurements at  $180^\circ$  are repeated multiple times. Some variations are seen. This introduces (one source of) systematic error and will be included in the further analysis.

$$\Delta \dot{C}_{\text{sys}} = 0.564 \quad (23)$$

Data after these corrections are plotted in figure. 7. Vertical error bars include statistical error and systematic error. Error of angle is estimated to be about 2 degrees.

A least squares fit of data using function in the form of (18) is carried out. Fitted function is drawn in blue in figure 7. Parameters are shown in table 4. One should emphasize that

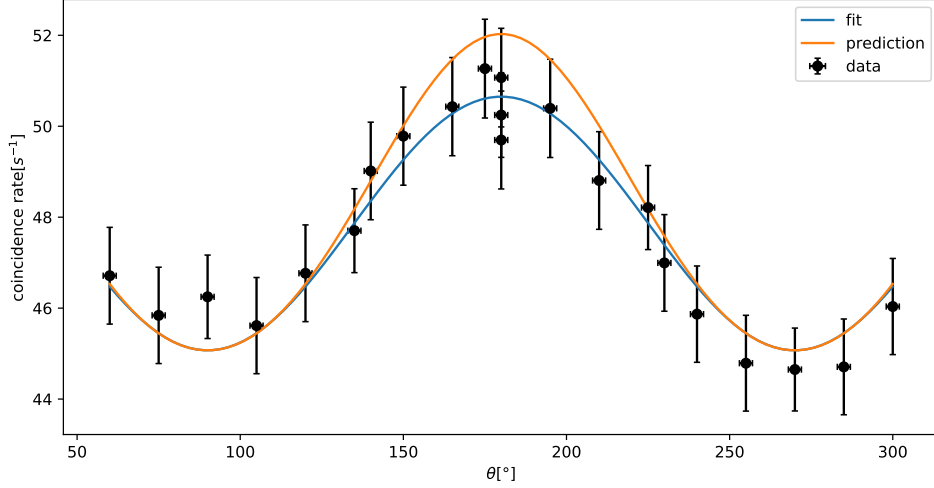


Figure 7: Angular correlation with fit and prediction

	fit	theory
$A$	$45.0721 \pm 0.2578$	
$B$	$0.1246 \pm 0.0310$	0.1213
$C$	$-0.0008 \pm 0.0289$	0.0330

Table 1: Parameters of the curve shown in figure 7 and their theoretical values after being "corrected" for finite size of detector

the errors in table 4 are only the diagonal entries of covariance matrix. There are still non-vanishing off-diagonal entries, i.e. variables are somehow correlated. This is the reason why drawing confidence intervals in figure 7 is not meaningful. Covariance matrix of these fitting parameters is

$$\Sigma_{ABC} = \begin{pmatrix} 0.06648601 & -0.00610261 & 0.00462504 \\ -0.00610261 & 0.00096016 & -0.00086438 \\ 0.00462504 & -0.00086438 & 0.00083277 \end{pmatrix} \quad (24)$$

Based on this value of  $A$ , we can plot the predicted function equation (20). Because of finite size of detector, prediction curve needs to be "corrected" by factor  $Q_k$  to correspond measured correlation curve. It is more convenient to apply this correction to fit curve than data points. Values of  $Q_k$  are taken from [2] with distance to source  $h = 5$  cm. Energy of  $\gamma$ -radiation in experiment is between 1 MeV and 1.5 MeV and only photopeaks are relevant. For convenience, mean values of  $Q_k$  of these two energies are used in calculation

$$Q_2 = 0.934, Q_4 = 0.792$$

Theoretical prediction with  $Q$  correction of fit parameters are also added in table 4.

It seems that prediction and measurement have at least OK agreement, only some deviation around  $180^\circ$  is present. But a closer look is necessary, since the fit parameters are correlated. For simplicity, we say that  $A$  has no correlation to other parameters and only its best-fit value is used. This will underestimate "distance" between theory and measurement. Taking only  $B$



and  $C$  components of equation (24), one can draw confidence intervals on parameter plane. In figure 8, one can see prediction value lie roughly  $4\sigma$  away from best-fit value, even though

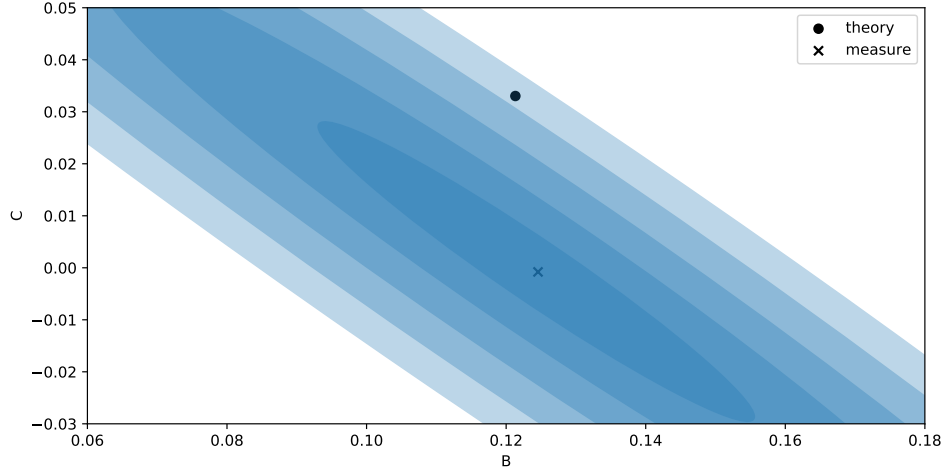


Figure 8: Regions on the plane  $(B, C)$  measured by experiment. Best-fit and theoretical prediction are included. The contours corresponds to  $1\sigma$ ,  $2\sigma$ ,  $3\sigma$ ,  $4\sigma$ ,  $5\sigma$  confidence intervals.

table 4 gives us roughly  $1\sigma$  accuracy.

Just as a consistency check and to better understand origin of deviation,  $B$  and  $C$  can be converted into  $\alpha$ ,  $\beta$  like before.

$$\begin{pmatrix} \alpha \\ \beta \end{pmatrix} = \begin{pmatrix} 1 & 1 \\ 1 & -1 \end{pmatrix} \begin{pmatrix} B \\ C \end{pmatrix} \quad (25)$$

	fit	theory
$\alpha$	0.1238	0.1544
$\beta$	0.1254	0.0883

Table 2: Prediction and measurement of  $\alpha, \beta$ . Here theoretical value has been corrected by  $Q$ -factor.

Results are in table 2. Their covariance matrix is

$$\Sigma_{\alpha\beta} = \begin{pmatrix} 6.416\,647\,49 \times 10^{-5} & 1.273\,956\,76 \times 10^{-4} \\ 1.273\,956\,76 \times 10^{-4} & 3.521\,699\,20 \times 10^{-3} \end{pmatrix}$$

Thus deviations are present at all angles, not e.g. only around  $180^\circ$  when only  $\alpha$  is off.

There is quite obvious asymmetry (with respect to  $180^\circ$ ) present in the angular correlation. Ideally, this should not be in data, or at least after being corrected by considering misalignment. To better see the difference, data points are plotted in figure. 9. From this, we can see that the asymmetry can be well explained by the errors.

They need to be converted to  $A_{kk}$  coefficients and then corrected for finite size of detectors. As written in equation (20), both  $A_{22}$  and  $A_{44}$  decides the values of  $B$  and  $C$  (need to scale

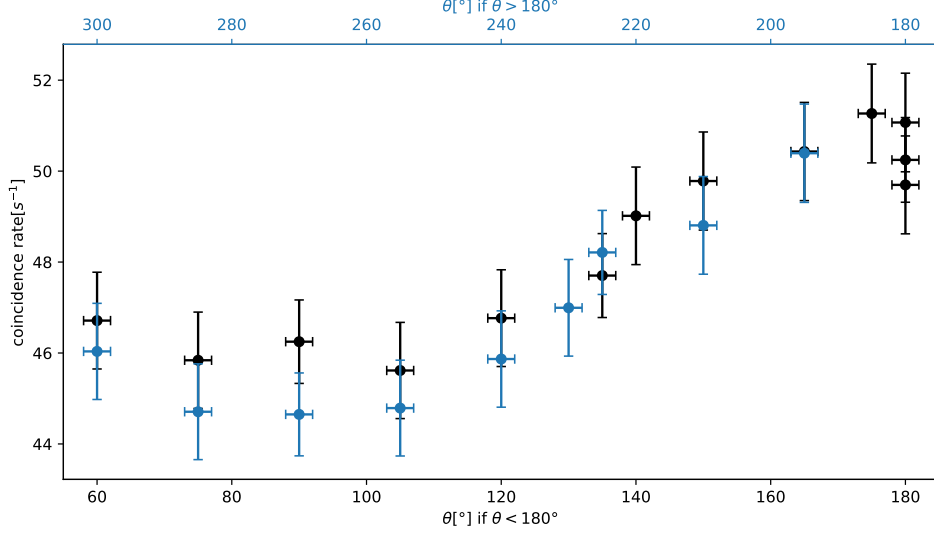


Figure 9: Angular correlation to see asymmetry. Color of data points correspond to the color of axis to use.

it, so that the constant term is unity!). Thus it involves finding the inverse of the matrix. The errors here are given without correlation considered, i.e. these are only diagonal entries of covariance matrix.

	fit with correction	theory
$A_{22}$	$0.0849 \pm 0.0057$	0.1020
$A_{44}$	$-0.0002 \pm 0.0063$	0.0091

Table 3: Measured coefficients after corrected for finite size of detectors and theoretical values

Fitting of angular correlation could also help us to exclude other cascades. From previous found values of  $B$  and  $C$ , one can conclude that 020, 121, 220, and 320 cascades are pretty much 100% excluded using coefficients provided by [3]. Alternatively, fit function can also only contain  $\cos^2 \theta$  term. This fit curve visually doesn't differ from the previous curve visually, as expected since  $C$  from previous fit is almost vanishing. New fit parameters are Comparing this

	fit
$A$	$45.0765 \pm 0.1969$
$B$	$0.1237 \pm 0.0077$

Table 4: Parameters using alternative fit function. Errors are just the diagonal entries of covariance matrix.

$B$  to values give in [3], the closest (positive) value is of 210 and 220 cascades with  $B = 3/7 \approx 0.43$ . Although  $Q$  correction is not included, we know for sure  $Q \sim 1$ , and measured value is no way near 0.43 (more than dozens of  $\sigma$ s away). Some negative values are numerically closer

to measured value. But from the plot, coefficient  $B$  is obviously positive. We can say for sure, measured angular correlation does not correspond to any other cascade listed in [3].

## 6 Discussion And Conclusion

In our experiment, we investigate nuclear properties of cobalt nuclei via angular correlation for that, firstly, we have set up gain of main amplifier ( $A_1$  and  $A_2$ ) and upper limit for the gain used in the set up. Then Constant Fraction Discriminator(CFD) threshold has to be adjusted to filtered events. Afterward, we insert a fixed delay into one fast branch and a variable delay in to another one. Then, We picked resolving time (25 ns) for the first measurement. Furthermore, to adjust the timing of the fast coincidence (FC) unit connect a gate and delay generator to the output of FC. After setting up all the apparatus, we measured the coincidence using two detectors—one of them is fixed and another one is movable— with varying angle between them. Then, we fitted the measured data with the theoretical prediction function and calculated the angular correlation coefficients  $A_{22} = 0.125 \pm 0.031$  and  $A_{44} = -0.001 \pm 0.029$ . The non zero values of these two angular correlation coefficients, importantly, provide strong evidence for an angular correlation between two gamma rays emitted in cascade of  $^{60}\text{Co}$ . These coefficients almost agree with the theoretical prediction within the error limit; however, there is little bit deviation from theoretical value, maybe, due to the errors in our measurements.

## References

- [1] Unknown. *Experiment description: Nuclear  $\gamma$ - $\gamma$  Angular Correlations*. 2019.
- [2] Kai Siegbahn, ed.  *$\alpha$ -,  $\beta$ -, and  $\gamma$ -Ray Spectroscopy*. Vol. 2. North-Holland Publishing Company, 1965.
- [3] E. L. Brady and M. Deutsch. “Angular Correlation of Successive Gamma-Rays”. In: *Physical Review* 78.5 (June 1950), pp. 558–566. DOI: 10.1103/PhysRev.78.558.
- [4] P.D. Stevenson. “Analytic angular momentum coupling coefficient calculators”. In: *Computer Physics Communications* 147.3 (2002), pp. 853–858. ISSN: 0010-4655. DOI: [https://doi.org/10.1016/S0010-4655\(02\)00462-9](https://doi.org/10.1016/S0010-4655(02)00462-9). URL: <http://www.sciencedirect.com/science/article/pii/S0010465502004629>.
- [5] Plasma Laboratory of Weizmann Institute of Science. *369j-symbol Calculator*. URL: <https://plasma-gate.weizmann.ac.il/369j.html>.
- [6] Robert Allan Wilson. “Directional correlation of the 346-136 keV gamma-gamma cascade in Ta181”. MA thesis. Portland State University. Department of Physics, 1969. URL: [https://pdxscholar.library.pdx.edu/open\\_access\\_etds/75/](https://pdxscholar.library.pdx.edu/open_access_etds/75/).
- [7] Hermann Kolanoski and Norbert Wermes. *Teilchendetektoren*. Springer Berlin Heidelberg, 2016.
- [8] Qwerty123uiop. *File:PhotoMultiplierTubeAndScintillator.svg*. 2013. URL: <https://commons.wikimedia.org/wiki/File:PhotoMultiplierTubeAndScintillator.svg>.
- [9] G. Iaci and M. Lo Savio. “A fast-slow coincidence system”. In: *Nuclear Instruments and Methods* 65.1 (1968), pp. 103–109. ISSN: 0029-554X. DOI: [https://doi.org/10.1016/0029-554X\(68\)90014-1](https://doi.org/10.1016/0029-554X(68)90014-1). URL: <http://www.sciencedirect.com/science/article/pii/0029554X68900141>.
- [10] Ortec. *Single-Channel Pulse-Height Analyzers*.
- [11] Canberra Elektronik. *Constant Fraction Discriminator: Model 1326, 1428\* Operating Manual*.
- [12] R.B.firestone. *Table of Isotopes*. 8th ed. Wiley, New York, 1996.
- [13] Traitor. *File:60Co gamma spectrum energy.png*. 2007. URL: [https://en.wikipedia.org/wiki/File:60Co\\_gamma\\_spectrum\\_energy.png](https://en.wikipedia.org/wiki/File:60Co_gamma_spectrum_energy.png).